Mutations of Tyrosine 537 in the Human Estrogen Receptor-α Selectively Alter the Receptor's Affinity for Estradiol and the Kinetics of the Interaction[†]

L. Zhong and D. F. Skafar*

Department of Physiology and Barbara Ann Karmanos Cancer Institute, Wayne State University School of Medicine, Detroit, Michigan 48201

Received December 3, 2001; Revised Manuscript Received January 30, 2002

ABSTRACT: Mutation of tyrosine 537 (Y537) of the human estrogen receptor-α (hERα) produces receptors having a range of constitutive activity, which suggests that this residue modulates the conformational changes of the receptor. We investigated the effect of several mutations at this position, to phenylalanine (Y537F), to serine (Y537S), and to glutamic acid (Y537E), on the hormone-binding properties of the receptor. The affinities of the wt, the Y537F mutant, and the Y537S mutant for estradiol were similar: $K_a = 2.2 \pm 0.2$, 3.9 ± 0.5, and 2.8 ± 0.4 nM^{-1}, respectively. By contrast, the affinity of the Y537E mutant for estradiol was reduced 10-fold, $K_a = 0.2 \pm 0.1$ nM^{-1}. All proteins bound [^{3}H]estradiol with a positive cooperative mechanism ($n_H = 1.7-1.9$), indicating they can form dimers. The wt receptor and the Y537S and Y537E mutants exhibited biphasic dissociation kinetics, which is also indicative of dimerization. Surprisingly, the half-lives of the slow component of the wt and the Y537E mutant were indistinguishable, 118 ± 3.4 and 122 ± 4.5 min, respectively, even though the affinity of the Y537E mutant for hormone was reduced 10-fold. The half-life of the slow component of the Y537S mutant was reduced to 96.5 ± 3.8 min. Molecular models were constructed and compared to identify changes in the structure that correlate with the observed effects on hormone binding. Local alterations in hydrogen bonding, the position of side chains, and the position of the peptide backbone were observed. Taken together, these results show that mutations at Y537 selectively alter the affinity and kinetics of hormone binding to the receptor, and are consistent with the idea that the estradiol−estrogen receptor interaction can follow more than one pathway.

The estrogen receptor-α (ER),[1] a member of the nuclear receptor superfamily, is a ligand-inducible transcription factor that mediates many of the actions of estrogen in target cells (*1*−*4*). Upon agonist binding, the ER undergoes conformational changes which lead to dissociation of heat shock proteins, dimerization, and binding to the DNA at estrogen response elements in regulated genes. The receptor enhances gene expression through interaction with coactivators such as AIB-1 and SRC-1 (*5*−*12*). Numerous factors regulate the activity of the ER, such as the type of ligand bound to the receptor, the phosphorylation state of the ER, and the presence, type, and activity of the coactivator proteins (*1, 4, 13*−*15*).

Like all the members of this superfamily, the ER is a multidomain protein. The ligand-binding domain (LBD) is located near the C-terminal end of the protein, and the DNA-binding domain is in the middle of the protein (*1*). The major regions that contain sequences necessary for activation of transcription are found within the N-terminal domain (AF-1) and within the ligand-binding domain (AF-2). The activity of AF-2 is dependent on ligand binding, whereas the activity of AF-1 does not require ligand, but can be regulated by phosphorylation of specific serine residues (*16*). Although the functions of AF-1 and AF-2 can be separated, substantial information indicates the two domains can act synergistically (*17*).

X-ray crystallographic structures of the LBD of the ER and other members of the nuclear receptor superfamily show that AF-2 is located in an α helix, termed "helix-12" (*18*−*24*). Tyrosine 537 (Y537) of the human ER is positioned at the Ncap of helix 12 in the agonist-bound protein (*21, 22, 25*) or within helix 12 at the N2 position in the antagonist-bound protein (*21, 22*). In the agonist-bound conformation, Y537 forms a hydrogen bond with asparagine 348 (N348) (*21, 22, 26*). Mutating Y537 to phenylalanine (Y537F) produced a receptor that responds to estradiol in transient transfection assays, but loses its hormone-binding activity more rapidly than the wt protein (*26*−*28*). Mutating Y537 to other amino acids resulted in receptors having different levels of constitutive transactivation, but which also respond to hormone stimulation (*27, 28*). Furthermore, a naturally

[†] Supported by the Barbara Ann Karmanos Cancer Institute, the National Cell Culture Center, NSF Grant IBN 9407376 (D.F.S.), EHS Center Grant ES 06639, NIH Grant 1RO1 DK56934-01A1 (D.F.S.), the Office of Reseach on Women's Health (NIH), and Department of Defense Grant DAMD 17-00-1-0498 (D.F.S.).

* To whom correspondence should be addressed at the Department of Physiology, Wayne State University School of Medicine, 540 E. Canfield Ave., Detroit, MI 48201. Phone: (313) 577-1550, FAX: (313) 577-5494, Email: dskafar@med.wayne.edu.

[1] Abbreviations: ERα, human estrogen receptor-α; K_a, association constant; AIB-1, amplified in breast-1; SRC-1, steroid receptor coactivator-1; LBD, ligand-binding domain; AF-1, activation function-1; AF-2, activation function-2; wt, wild type; *Sf9*, *Spodoptera frugiperda* -9; MOI, multiplicity of infection; TDEG Tris−dithiothreitol−ethylenediaminetetraacetic acid−glycerol; PMSF, phenylmethylsulfonyl fluoride; E_2, 17β-estradiol; DES, diethylstilbestrol; n_H, Hill coefficient; RAR, retinoic acid receptor; PBS, phosphate-buffered saline; RMSD, root-mean-square derivative.

10.1021/bi0121095 CCC: $22.00
Published on Web 03/06/2002

occurring ER mutant in which the Y537 is replaced by asparagine (Y537N) was isolated from a patient having metastatic, tamoxifen-resistant breast cancer (*29*). This Y537N mutant, when transfected into mammalian cells, exhibited constitutive activity equal to or even greater than that of the hormone-stimulated, wt hERα (*29*, *30*). Thus, there is substantial evidence that Y537 plays a critical role in the structure and function of the hERα.

In this study, we have investigated the role of Y537 in the affinity and kinetics of hormone binding to the ER. Y537 mutants were generated in which Y537 was substituted by phenylalanine (Y537F), glutamic acid (Y537E), and serine (Y537S) and were expressed as histidine-tagged fusion proteins in *Sf9* insect cells using a baculovirus vector. These mutants were selected because they exhibit a range of constitutive activity, from equal to the wt receptor (Y537F), to moderately increased (Y537E), and to substantially increased (Y537S) (*27*, *28*). We then measured the affinity for estradiol, and the dissociation kinetics of estradiol from these mutant receptors. We have also used molecular modeling of the mutated receptors to understand how the mutations could affect the structure of the ER LBD and its interaction with ligand. Our results show that mutations at Y537 can have selective effects on the affinity of the receptor for ligand and the kinetics of the interaction.

EXPERIMENTAL PROCEDURES

Materials. The human estrogen receptor cDNA (HEG0-pSG5) was a generous gift from Dr. Pierre Chambon and Dr. Hinrich Gronemeyer (*31*). The Altered Sites II in vitro mutagenesis kit was purchased from Promega (Madison, WI). *Sf9* insect cells, Bac-N-Blue transfection kit, and Baculovirus protein expression kit were purchased from Invitrogen (San Diego, CA). Ovalbumin was purchased from Sigma (St. Louis, MO). Anti-hER antibody Ab-6 was obtained from NeoMarkers (Fremont, CA). 17β-[6,7-^{3}H(N)]Estradiol was purchased from DuPont/New England Nuclear (Boston, MA).

Site-Directed Mutagenesis of the hER. Oligonucleotide site-directed mutagenesis of the ER was performed according to the manufacturer's instructions (Promega). A 786 bp fragment of the wt hERα cDNA including the codon for Y537 was subcloned from HEG0-pSG5 by digesting with *Eco*RI and *Hin*dIII restriction endonucleases and ligated into the mutagenesis vector pALTER1 (Promega) to generate hER-pALTER1. Three 28 bp oligonucleotide primers were obtained from Operon (Alameda, CA), in which the sequence of each primer was matched to the cDNA sequence of the ER, with the codon for position 537 in the center. These primers contained altered sequences in which the tyrosine 537 (TAT) was changed to phenylalanine (TTT), glutamic acid (GAT), or serine (TCT). The oligonucleotide primers were annealed to the hER-pALTER1 single-stranded DNA along with two antibiotic-resistance-altering primers (the tetracycline knockout primer and the ampicillin repair primer, provided by Promega) in the presence of T4 DNA ligase, T4 DNA polymerase, and dNTPs to synthesize the mutated DNA strand. Mutant colonies were selected from LB plates containing 125 μg/mL ampicillin. All three mutants were confirmed by DNA sequencing. The ER cDNA fragments containing the mutation were excised from the mutagenesis plasmid and replaced into the HEG0-pSG5 plasmid to generate the full-length Y537E, Y537F, and Y537S mutant ERs in pSG5.

Transfection and Expression of the ER in Sf9 Cells. The wt and all three Y537 mutant ERs were excised from their respective pSG5 vectors by digestion with *Eco*RI and *Msl*I and ligated into the pBlueBacHis2B vector using standard molecular biological techniques to generate transfer plasmids for generation of recombinant baculovirus. The correct insertions were confirmed by DNA sequencing.

The transfer plasmids containing the wild-type and the Y537F, Y537E, and Y537S ERs were cotransfected with the linear viral DNA AcMNPV by the technique of cationic liposome-mediated transfection using procedures suggested by the manufacturer (Invitrogen). Identification of recombinant virus and generation of a high-titer virus stock were carried out using procedures suggested by the manufacturer (Invitrogen). The recombinant wt and mutant ER proteins were expressed by infecting *Sf9* cells (10^6 cells/mL) with the corresponding high-titer virus stocks at an MOI of 5. The time required for optimal expression of each protein was determined in a preliminary set of experiments. After expression, the cells were washed with PBS and pelleted in 50 mL aliquots. The pellets were stored at −80 °C. The presence of the ER and its molecular weight were confirmed by Western immunoblotting.

Preparation of the wt and Mutant ERs from Sf9 Cells. An *Sf9* cell pellet containing expressed ER was lysed on ice with a Wheaton Potter−Elvehjem tissue grinder (10−15 strokes) in buffer consisting of 40 mM Tris, 5 mM DTT, 0.1 mM EDTA, 300 mM NaCl, 15% glycerol, pH 7.5 (TDEG + salt buffer), 20 mg/mL ovalbumin, and final concentrations of 0.4 mM PMSF, 47 μg/mL leupeptin, 1 μg/mL pepstatin, and 2 μM E64. The cell extracts were clarified by centrifugation at 220000*g* for 30 min at 4 °C.

Equilibrium Binding of Estradiol to the wt and Y537 Mutant ERs. Equilibrium binding experiments were carried out using procedures similar to those described by Sasson and Notides (*32*). Preliminary experiments were conducted to determine the time necessary for each mutant to achieve equilibrium, and to ensure that each mutant was stable during the assay (data not shown). Aliquots (200 μL) of the cell extracts containing wild-type or Y537 mutant ERs were prepared as above and then were incubated with increasing concentrations of [^{3}H]estradiol, in duplicate, for 2 h at 25 °C to reach equilibrium. The nonspecific binding was determined in a parallel set of incubations, in duplicate, containing a 200-fold molar excess of unlabeled estradiol. The total concentration of [^{3}H]estradiol in each tube was determined by removing an aliquot (50 μL) of the mixture from each tube at the end of the incubation, followed by liquid scintillation counting. Free steroid and bound steroid in the remaining mixture were separated by dextran/charcoal assay (*32*). Inactivation of the hormone-free receptor was routinely measured in each experiment and was less than 10%.

The affinity of the receptor for estradiol was determined from the limiting slope of the Scatchard plot (*33*), which yields the affinity of binding to the second site (*34*). The Hill coefficient (*35*) was obtained by nonlinear regression analysis of the bound vs free ligand using the program Enzfitter.

Dissociation Kinetics of [^{3}H]Estradiol from the Y537 Mutants and wt ERs. The dissociation of estradiol from the ER was studied using procedures similar to Weichman and Notides (*36, 37*). Cell extracts from the *Sf9* cells containing overexpressed wt and Y537 mutant ERs were prepared as above. Then 6 mL of each cytosol was incubated with a saturating concentration of estradiol, 20 nM [^{3}H]E_2, for 60 min at 25 °C. The unbound steroid was absorbed from the cytosol by incubation with 3 mL of dextran/charcoal TDE buffer suspension for 10 min at 0 °C. The charcoal then was pelleted by centrifugation for 5 min at 1000*g*. At the end of the centrifugation, the supernatant was removed, 10 μM unlabeled E_2 was added to it, and the incubation was continued at 25 °C. At the times indicated (0, 1, 2, 3, 5, 7, 10, 15, 20, 30, 45, 60, 90, 120 min), duplicate 0.2 mL aliquots were removed. Free steroid and bound steroid were separated by dextran-coated charcoal assay of each aliquot as described above. The inactivation of the [^{3}H]E_2-bound receptors was measured in the absence of the excess unlabeled E_2 in a parallel incubation and was less than 10%.

Data were analyzed using GraphPad PRISM. For proteins exhibiting biphasic dissociation kinetics (wt receptor, Y537S, Y537E), the equation for two-component exponential decay was used. The values of the fast component of the dissociation curve were corrected by subtracting the contributions of the slow component. The slope of the slow component was extrapolated to zero time, and its value at each time point was subtracted from the experimental value of the fast component. All data were graphed semilogarithmically with the *Y*-axis as the percentage of bound [^{3}H]E_2 compared with the value at $t = 0$ (100%).

Molecular Modeling. Molecular modeling was carried out using Biopolymer and Discover within InsightII 98 (Molecular Simulations, Inc.) using a Silicon Graphics O2 workstation and the cvff force field. The models were based on the coordinates of residues 305−550 of the "A" chain of the DES-bound hERα LBD (3ERD, *22*). All modeling was carried out in the presence of DES and one crystallographic water near the ligand-binding pocket of the protein, without constraints. Residues in the crystallographic structure of the wt protein that had incomplete side chains (residues 305, 306, 330, 332, 335, 437, 460−470, 531, 548, 549) were completed by replacement, hydrogens were added (pH 7.0), and the model was subjected to 100 rounds of steepest descent minimization with charges, but without Morse potentials and cross-terms, followed by conjugate gradient minimization with charges, Morse potentials, and cross-terms until the maximum RMSD was less than 0.001. The mutant ERs were constructed by replacing Y537 in the coordinates of the crystallographic structure of the wt protein with the indicated amino acid, followed by minimization as above.

RESULTS

Equilibrium Binding of [^{3}H]E_2 to the wt and Y537 Mutant ERs. We first determined whether mutations at Y537 alter the affinity of the ER for estradiol. Preliminary experiments were carried out to test the stability of each receptor during the assays and to determine the length of time necessary for each receptor to achieve equilibrium at the lowest and highest concentrations of ligand. All receptors were stable in buffer containing ovalbumin carrier protein and 300 mM NaCl at 25 °C for up to 2 h, and equilibrium was achieved under these conditions in less than 2 h (not shown). Inactivation of the hormone-free receptor was routinely measured in each experiment and was less than 10%.

The value of the affinity of estradiol binding to the wt ER we obtained, $K_a = 2.2$ nM^{-1}, is consistent with previously reported values for the human ER (*26, 38*). The hormone-binding affinities of the wt ER, the Y537F, and the Y537S mutant did not differ (Figure 1; Table 1). Most strikingly, the Y537E mutant exhibited a 10-fold lower affinity for estradiol than the wt ER (Figure 1; Table 1).

We also measured the Hill coefficient of the binding of [^{3}H]estradiol to each receptor. The Hill coefficient is an indicator of the binding mechanism between the receptor and the ligand; a Hill coefficient of 1 characterizes a noncooperative binding mechanism, indicating either that the protein is monomeric or that site−site interactions do not occur (*39*). A Hill coefficient greater than 1 is indicative of a positive cooperative binding mechanism and site−site interactions in which binding of ligand to one subunit favors binding to a second subunit (*39*). Note that a cooperative binding mechanism is diagnostic of an oligomeric protein (*39*).

The calf uterine estrogen receptor has been previously shown to bind [^{3}H]estradiol with a positive cooperative mechanism, having a Hill coefficient of approximately 1.6 (*40*); dilution of the estrogen receptor eliminates positive cooperativity, leading to a Hill coefficient near 1 (*40*). The value of the Hill coefficient of estradiol binding to the wt hERα we obtained, $n_H = 1.9$, is consistent with previously reported values for the human ER (*26, 38*). In our experiments, each receptor exhibited strong positive cooperativity, having Hill coefficients for the binding of [^{3}H]estradiol between 1.6 and 1.9 (Figure 1; Table 1). These results show that mutation of Y537 did not eliminate site−site interactions or dimerization.

Dissociation of [^{3}H]E_2 from the wt and Mutant ERs. Analysis of the dissociation kinetics of the estrogen receptor has been used to detect changes in the conformation of the receptor (*36, 37*). The calf uterine estrogen receptor exhibits biphasic dissociation kinetics (*36, 37*). Dilution of the receptor increases the proportion of the receptor exhibiting the fast rate of dissociation, and eliminates the slow rate of dissociation (*37, 41*). These and other results have shown that the fast component of the [^{3}H]E_2 dissociation curve corresponds to the lower affinity, monomeric, state of the calf receptor and the slow component corresponds to the higher affinity, dimeric, state of the receptor (*36, 37*). Since the amino acid sequences of the ligand-binding domains of the bovine and human estrogen receptors are 98% identical (*42, 43*), the human ER is expected to exhibit similar properties.

Like the calf uterine estrogen receptor, the baculovirus-expressed, histidine-tagged wt hER exhibited two-component dissociation kinetics (Figure 2). The Y537E and Y537S mutants also exhibited two-component dissociation kinetics (Figure 2). Because of the high degree of identity between the bovine and human ER, it is reasonable to attribute the fast dissociating components of the wt, Y537E, and Y537S ERs to ER monomers, and the slow dissociation component to ER dimers. Dimerization of the wt and mutant ER is also

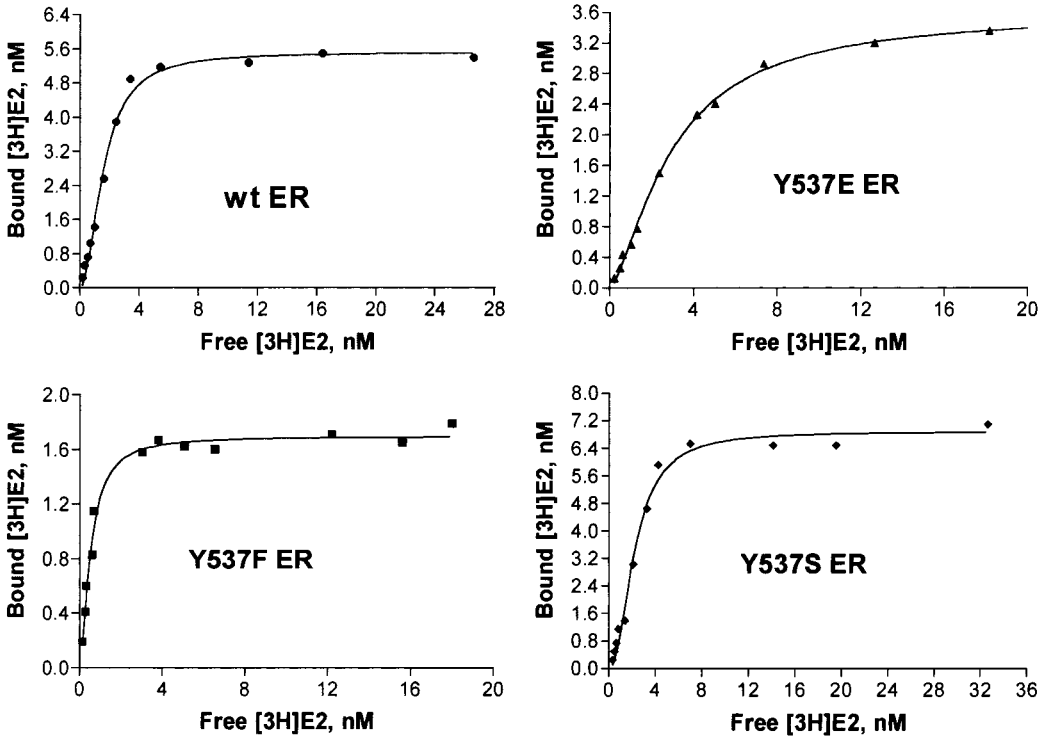

FIGURE 1: Equilibrium binding of the wt ER and the Y537 mutants with [^{3}H]E_2. Extracts of *Sf9* insect cells containing the overexpressed wt ER and the Y537 mutants were prepared and incubated with [^{3}H]E_2 as described under Experimental Procedures at 25 °C in buffer containing 300 mM NaCl and 20 mg/mL ovalbumin carrier protein. These data are representative of 3−5 independent experiments, each carried out in duplicate.

Table 1: Affinity of the Wild-Type and Mutant hERα for [^{3}H]Estradiol[a]

receptor	association constant, K_a (nM^{-1})	Hill coefficient, n_H
wt	2.19 ± 0.20	1.87 ± 0.07
Y537F	3.90 ± 0.53	1.68 ± 0.07
Y537E	0.20 ± 0.11*	1.76 ± 0.03
Y537S	2.80 ± 0.41	1.93 ± 0.07

[a] Extracts of *Sf9* insect cells infected with recombinant baculovirus to express the indicated ER were incubated with increasing concentrations of [^{3}H]estradiol for 1.5 h at 25 °C; nonspecific binding was measured in a parallel set of incubations containing a 200-fold molar excess of unlabeled estradiol. Free steroid and bound steroid were separated by dextran-coated charcoal assay and were measured using liquid scintillation counting. The Hill coefficient was calculated by using Lotus 1-2-3 and Enzfitter (Elsevier-Biosoft); the K_a was obtained from the limiting slope of the Scatchard plot. Data are expressed as mean ± SEM of three to five independent experiments, and were analyzed using the *t*-test to compare with the wt ER values. *, $p < 0.005$.

consistent with the observation that each receptor bound [^{3}H]estradiol with a positive cooperative binding mechanism (Table 1).

For the wt ER, the half-life of the slow component was 118 ± 3.4 min (Table 2). This value was indistinguishable from the half-life of the slow component for the Y537E receptor, 122 min (Table 2). The half-life of the slow phase of dissociation for the Y537S mutant was reduced only slightly, 18%, from the value for the wt protein, 96.5 vs 118 min (Table 2). We also measured the effects of the Y537E and Y537S mutations on the fast component of the dissociation: the half-life of this phase was increased from 13.9 min in the wt to 20.6 min in the Y537E mutant, a 48% increase, and was decreased to 8.9 min in the Y537S mutant, a 36% decrease (Table 2). Overall, the Y537E and Y537S mutations

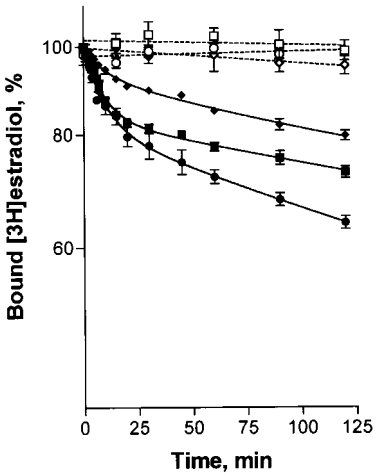

FIGURE 2: Dissociation rate of [^{3}H]E_2 from the wt and the Y537 mutant ERs. Cell extracts containing the wt (squares), Y537S (circles), or Y537E (diamonds) receptor were prepared and incubated with a saturating concentration of [^{3}H]E_2 for 1 h at 25 °C. The extracts were treated with dextran-coated charcoal, and a 200-fold molar excess of unlabeled E_2 was added. Aliquots were removed at the indicated times, and bound [^{3}H]E_2 was measured by charcoal assay (closed symbols). Receptor inactivation was measured in parallel incubations containing only labeled [^{3}H]E_2 and which were not subject to the first DCC treatment (open symbols). Less than 10% of the hormone-binding activity was lost during incubations. The data are the mean ± SEM of four independent experiments, each carried out in duplicate. Where error bars are not shown, the bar is less than the size of the symbol.

had little or no effect on the half-life of the slow component of the dissociation curve. These same mutations exerted larger effects—and in opposite directions—on the half-life of the fast component of the dissociation curve. Most interestingly, the 10-fold reduced affinity of the Y537E

Table 2: Dissociation of [^{3}H]Estradiol from the Wild-Type and Mutant hERα[a]

receptor	fast component half-life (min)	slow component half-life (min)
wt	13.9 ± 0.6	118 ± 3.4
Y537E	20.6 ± 0.7	122 ± 4.5
Y537S	8.9 ± 0.9	96.5 ± 3.8

[a] The dissociation of [^{3}H]estradiol from the wt and Y537 mutant ERs was measured at 25 °C for up to 2 h. For the wt, Y537E, and Y537S mutants, data were analyzed using the equation for two-phase exponential decay using GraphPad PRISM. The results are the mean ± SEM of four independent experiments, each performed in duplicate.

mutant for estradiol cannot be accounted for by a change in the rate of dissociation of the ligand from the receptor.

Molecular Modeling of the wt and Mutant ERs. Molecular models of the ligand-binding domain of the wt and the Y537E, Y537S, and Y537F mutant ERs were constructed using Biopolymer and Discover (Molecular Simulations, Inc.) and compared to identify changes in the structure. Models were based on the coordinates of residues 305−550 of the "A" chain of the DES-bound hERα LBD (3ERD, *22*). All modeling was carried out in the presence of DES and one crystallographic water, without constraints. This crystallographic water was retained during modeling because it is located within the protein, near the ligand-binding pocket, and hydrogen bonds with the ligand (*21*, *22*). The crystallographic water occupies a "window" in the LBD through which part of the ligand can be seen. A similar window containing a water molecule is observed in the crystallographic structures of the ligand-binding domains of the TR, the RAR, the AR, and the PR (*18*−*20*, *23*, *24*, *44*); it has been proposed as the pathway for exit of the ligand from the thyroid receptor (*19*) and the RAR (*45*).

No changes in the position of the DES ligand and the crystallographic water were observed in any of the mutants after energy minimization. The water remained within the "window" of the LBD, even though it was not constrained during minimization. All of the substitutions at Y537 produced only local changes in the conformation of the ER.

Since Y537 is hydrogen-bonded with asparagine 348 (N348) in the wt protein, we examined the hydrogen bonding of these residues. The side chain of aspartic acid 351 (D351) is nearby in the crystallographic structure and makes a hydrogen bond with the amide hydrogen of leucine 540 (L540) at the start of helix 12; its position was investigated as well. Finally, since serine and glutamic acid have shorter side chains than tyrosine, we examined whether the peptide backbone was displaced.

In the wt protein, Y537 forms a hydrogen bond with N348, while D351 forms a hydrogen bond with the amide hydrogen of L540 at the beginning of helix 12; there is no hydrogen bond between Y537 and D351 (Figure 3). In the Y537S mutant, D351 has moved away from helix 12, and a hydrogen bond network involving the side chains of S537, N348, and D351 has been formed (Figure 3). In the Y537E mutant, the hydrogen bond between D351 and the amide hydrogen of L540 is retained (Figure 3, left panels). Like the wt tyrosine, the Glu537 side chain forms a hydrogen bond with N348; however, the glutamic acid side chain is closer to helix 11 than the wt tyrosine (Figure 3, right panels). The retention of a hydrogen bond involving position 537 in the models of

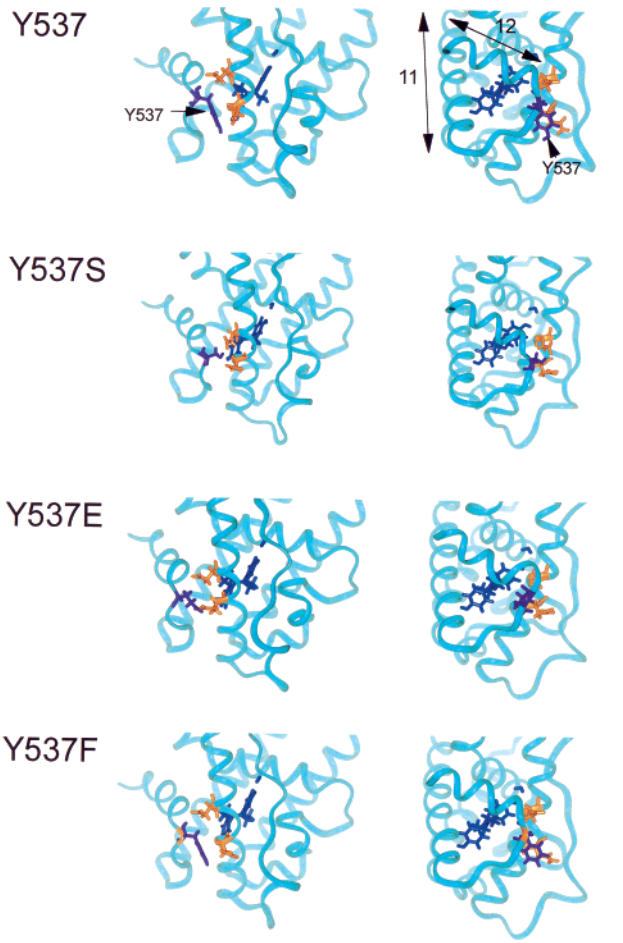

FIGURE 3: Structural alterations near position 537 in the minimized models of the wt and mutant hERα LBDs. Molecular modeling was carried out as described under Experimental Procedures. The peptide backbone is shown as a ribbon in cyan; the DES ligand and the crystallographic water are shown in dark blue; the residue at position 537 is shown in purple; and D351 and N348 are shown in orange. Y537 is also labeled in the model of the wt receptor by arrows. In all panels, D351 is closer to the top, and N348 is closer to the bottom. Helix 12 and helix 11 are labeled in the right-hand panel of the model of the wt receptor. Two views of the indicated complexes are shown. In the views on the left, helix 11 is in the back and helix 12 is on the left; in the views on the right, helix 11 is on the left and helix 12 is in the front.

the Y537S and Y537E mutants, coupled with the smaller and more polar nature of the substituted side chains compared with the wt tyrosine, is consistent with the greater stability and decreased tendency toward aggregation of these mutants when compared with the wt protein and the Y537F mutant (*26*; Zhong and Skafar, unpublished observations). It is also tempting to speculate the hydrogen bond network observed in the model of the Y537S mutant may be related to the extraordinarily high constitutive activity of this protein.

Though both serine and glutamic acid can form hydrogen bonds, their side chains are shorter than the tyrosine side chain. Displacement of the peptide backbone in the vicinity of the Y537 substitution was observed for the Y537E and Y537S mutants (Figure 3); interestingly, the displacements were in the opposite direction for the two mutants. In the Y537E mutant, the backbone is pulled toward helix 11; in the Y537S mutant, the backbone is pulled away from helix 11 (Figure 3, right panels). The changes in the position of the side chain of residue 537 and the peptide backbone at

Table 3: Summary of the Effects of Mutations at Y537 on hERα[a]

	receptor			
property	Y537 (wt)	Y537F	Y537S	Y537E
affinity for E2	high	high	high	reduced
E2 binding mechanism	cooperative	cooperative	cooperative	cooperative
dissociation kinetics	biphasic	monophasic[b]	biphasic	biphasic
hydrogen bond partner	N348[c,d]	none	network with N348, D351	N348

[a] Data from this report except where indicated. [b] (*26*). [c] (*21*). [d] (*22*).

that position in the models of the two mutants lead to opening of the triangle formed by helix 12, the bottom of helix 11, and the loop between them in the Y537S mutant, and closing of that same triangle in the Y537E mutant (Figure 3).

The Y537F mutant (Figure 3), lacking a phenolic hydroxyl, cannot form a hydrogen bond with N348. It does not exhibit significant alterations in the peptide backbone after minimization, and the hydrogen bond between D351 and the amide hydrogen of L540 in helix 12 is retained. However, the side chain of N348 has reoriented so that the distance between the side chains of amino acid 537 and N348 increases from 2 Å in the wt structure to 4.9 Å in the Y537F mutant (Figure 3, left panels). The net loss of a hydrogen bond and subsequent displacement of the F537 and N348 side chains in the model of the Y537F mutant are consistent with the decreased stability and greater tendency toward aggregation of the Y537F mutant compared with the wt protein (*26*, Zhong and Skafar, unpublished observations).

DISCUSSION

The role of Y537 in the conformation changes and activity of the hERα remains incompletely understood. Biologically, mutations of the hERα at Y537 produce receptors having a range of constitutive activity, from equal to that of the wt receptor (Y537F), to moderately increased (Y537E), to substantially increased (Y537S) (*27*−*30*). Biochemically, Y537 occupies an interesting position—the Ncap—at the start of helix 12 in the agonist-bound hERα and forms a hydrogen bond with N348, thereby bridging helix 12 and helix 3 (*21*, *22*, *25*). We selected mutations that exhibit a range of constitutive activity of the receptor, and examined their hormone-binding properties and energy-minimized models to understand the role of Y537 in the structure and function of the hERα. Our results provide strong evidence that mutations of tyrosine 537 in the hERα, leading to altered hydrogen bonding at this position, selectively alter the affinity of the ER for hormone and the kinetics of the interaction.

Surprisingly, the presence or absence of a hydrogen bond involving residue 537 was not correlated with the affinity of the ER for E2 (Table 3). The Y537F mutant, which cannot form a hydrogen bond, binds E2 at least as tightly as the wt ER, while the Y537E mutant, which modeling indicates retains the hydrogen bond with N348, has a 10-fold lower affinity for E2 than the wt protein. Moreover, all tested mutants of Y537—Y537F, Y537S, and Y537E—retained a cooperative binding mechanism for estradiol, indicating that site−site interactions were not impaired (Tables 1 and 3). Thus, a hydrogen bond between residue 537 and N348 is not required for either high-affinity binding to E2 or site−site interactions of the ER.

Alterations in hydrogen bonding by mutation did correlate with changes in the dissociation kinetics of E2 from the ER (Table 3). Those substitutions predicted by modeling to retain a hydrogen bond involving residue 537—Y537S and Y537E—retained the biphasic dissociation kinetics of the wt ER (Table 3); the Y537F mutant, when analyzed under the same conditions used in this report, exhibits monophasic dissociation kinetics (*26*). This provides strong evidence that a hydrogen bond involving residue 537 is required for the biphasic dissociation kinetics of the ER.

The observation that the Y537F mutant exhibits monophasic dissociation kinetics (*26*) whereas the wt and the Y537S and Y537E mutants exhibited biphasic dissociation kinetics (Figure 2; Table 2) is something of a puzzle. Substantial evidence exists that the biphasic kinetics of the ER are produced by the monomeric and dimeric forms of the receptor (*36*, *37*, *41*). This would imply the Y537F mutant exists either solely as monomer or as dimer, and the Y537F mutant would be expected to display an off-rate similar to either the fast or the slow phase of dissociation of the wt protein. However, the observed dissociation rate, $t_{1/2} = 65.4$ min, is different from either the fast or the slow phases of the wt ER, 13.9 and 118 min, respectively. Furthermore, if the mutant were monomeric, a Hill coefficient near 1 would be expected in equilibrium binding experiments; we and others observed that the Y537F mutant exhibits positive cooperativity, $n_H = 1.7$ (*26*; Table 1). Thus, a change in the dimerization cannot account for this observation.

Another puzzling observation is that although the Y537E mutant exhibits a 10-fold lower affinity for estradiol than the wt protein, the values of the slow component of the dissociation rate of the two proteins are indistinguishable (Table 2). This implies that the mutation to glutamic acid specifically alters the rate of association of the ligand with the receptor. One explanation is that the tyrosine to glutamic acid mutation may selectively destabilize the conformation of the hormone-free receptor, favoring the formation of the active conformation of the receptor. This is consistent with the observations that the Y537E mutant has moderately increased constitutive activity in transient transfection assays (*27*, *28*). However, if this were the case, the Y537S mutant, which displays dramatically increased constitutive activity (*27*), would also be expected to exhibit a greatly decreased affinity for hormone, which neither we nor others have observed (Table 1; *46*). Thus, relative destabilization of the inactive conformations of the Y537E and Y537S receptors cannot explain the effects of these mutations on the activity of the receptor.

It has been suggested that ligand binding requires an "open" conformation of the ER (*46*), and that the Y537F mutation favors a more "open" conformation of the ER (*26*, *27*). Fluorescence studies also suggest that a partially unfolded intermediate of the ER LBD facilitates ligand binding and release (*47*). Neither study, however, addressed the detailed pathway through which the ligand enters or exits the ER.

Two models based on molecular dynamics studies have been advanced to explain how the ligand may bind to, and dissociate from, a related protein, the retinoic acid receptor. In the mouse-trap model (*48*, *49*), the unliganded receptor has an open conformation, so that helix 12 extends away from the body of the LBD; binding of the ligand causes the

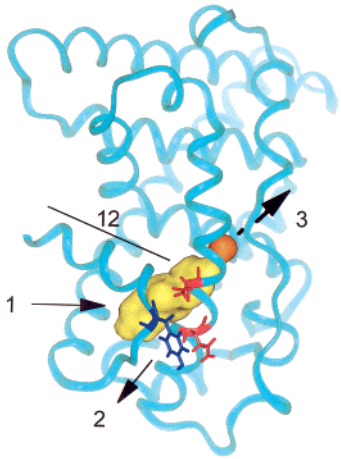

FIGURE 4: Possible binding and dissociation pathways for the interaction of ligand with the hERα LBD. Molecular modeling was carried out as described under Experimental Procedures. The peptide backbone is shown as a ribbon in cyan. Y537 is in blue. N348 and D351 are in red. DES (Connolly surface) is in yellow, and a crystallographic water (Connolly surface) is in orange. The position of helix 12 is indicated by a line. Pathways for ligand binding and dissociation are indicated by arrows, and are numbered according to Kostzin et al. (*45*) for the RAR.

reorientation of helix 12 over the ligand. In this model, dissociation of the ligand proceeds by the reverse of the binding process: helix 12 moves away from the body of the LBD, and the ligand exits following the same pathway it used to enter. The effects of the Y537F mutation are well-explained by this model: loss of the hydrogen bond between helix 12 and helix 3 would increase the flexibility of the ER, speeding both the association and dissociation of ligand. It is, however, difficult to account for the effect of the Y537E mutation on the association, but not dissociation, of ligand with this model. Moreover, ERα contains ~45 amino acids C-terminal to the ligand-binding domain, the F domain, that stabilizes the position of helix 12 in the ligand-bound receptor (*50*). Since the first step in the dissociation of ligand from the receptor in the mouse-trap model is the movement of helix 12, the presence of the F domain in the ER makes that model less plausible. In the second, "alternative pathways", model (*45*), formation of an open conformation is not required for either ligand binding or exit: movement of side chains allows the ligand to "wriggle" into and out of the binding cavity. Most importantly, the second model suggests that the ligand follows different pathways for binding to and dissociating from the receptor. This provides a simple explanation for the ability of the Y537E mutant to alter the association rate, but not the dissociation rate, of ligand from the receptor.

In the alternative pathways model of the retinoic acid receptor, three potential pathways through which the ligand could bind to or dissociate from the receptor were identified and tested (*45*). Similar potential pathways can be identified in the ER LBD (Figure 4). Like path 1 in the RAR, helices 11 and 12 in the ER are connected by a flexible loop, and a small part of the ligand is visible in the crystallograpic structure and energy-minimized model (Figures 3 and 4). A path underneath helices 11 and 12, corresponding to path 2 in the RAR, is also apparent in the DES-bound ER LBD (Figure 4). Finally, a "window" corresponding to path 3 of the RAR and containing a crystallographic water molecule is apparent in the crystallographic structures of the agonist-bound ER LBD (*21*, *22*) and the minimized model (Figures 3 and 4). Within the window, the ER has an arginine (R394) where the RAR has a lysine (K236). Position 537 in the ER is close to paths 1 and 2, but not path 3 (Figure 4).

Kostzin et al. suggested that retinoic acid enters the RAR LBD via path 1 and exits via path 3 (*45*). Path 2 was not energetically favorable (*45*). Since position 537 in the ER is close to the putative binding pathway (path 1), but not the dissociation pathway (path 3), this provides a simple explanation for the selective effect of the Y537E mutation on the association rate while leaving the dissociation rate unaltered (Figure 4).

The existence of alternative dissociation pathways can also explain the altered kinetics of hormone binding to the Y537F ER mutant and its retention of a high affinity for estradiol (*26*; Table 1). The uncompensated loss of the hydrogen bond between Y537 and N348 leads to separation of these side chains (Figure 3), as well as greater movement in this region of the modeled protein (Skafar, unpublished observations). Since position 537 is close to paths 1 and 2, this could not only facilitate binding through either path, but also allow the use of paths 1 or 2, rather than path 3, for dissociation.

Our modeling studies support the idea of separate association and dissociation pathways for ligand. In the Y537S model, movement of the peptide backbone and rearrangement of the side chains of S537, N348, and D351 open up the region near path 1; in the Y537E model, the peptide backbone and side chains have rearranged and impede path 1; in the Y537F model, the side chains of 537F and N348 have separated, which could facilitate binding through either path 1 or path 2 (Figures 3 and 4). Note that only local effects on conformation were observed in the models, so that in each model path 3 has not been altered.

Although the alternative pathways model can account for the effects of the mutations on the hormone-binding properties of the ER and is consistent with our modeling data, it is not entirely satisfactory since it does not account for experimental data that ligand binding to the ER involves a more open conformation of the receptor (*46*, *47*). Also, none of the proposed models explicitly addresses the link between receptor dimerization and its dissociation kinetics. We suggest ligand binding and dissociation are best explained using aspects of each proposed model. Ligand enters an open conformation of the ER LBD via one pathway; the monomeric ligand−receptor complex thus formed has rapid association and dissociation kinetics. Upon dimerization, the most stable, fully active conformation of the receptor is formed; because of conformation changes in the receptor due to dimerization, the ligand exits from the dimer by a different pathway and exhibits a much slower dissociation rate. A key point of this model is that formation of the fully active, slowly dissociating, most stable conformation of the ER requires not only ligand binding but also receptor dimerization. Mutation of Y537 to phenylalanine allows greater movement near the start of helix 12, facilitating the association of ligand and also permitting the ligand to dissociate following the same pathway, even in the receptor dimer. Mutation of Y537 to glutamic acid impedes the association of ligand, but has no effect on its dissociation from the dimer because dissociation follows a different pathway. Additional data, including structures of the full-length hormone-free and

hormone-bound ER in its different oligomeric states, will be needed to fully test these ideas.

Our finding that the Y537F mutant binds estradiol with high affinity and cooperativity provides additional strong evidence that phosphorylation of this tyrosine is not essential for hormone binding and dimerization (*51*−*54*). Our findings are also consistent with other reports that the Y537F mutant and its mouse receptor equivalent exhibit a similar affinity for hormone as the wt ERα (*26*, *28*). Other laboratories have used transient transfection in COS cells or expression in bacterial cells to obtain receptor for equilibrium and kinetic studies of the ER (*28*, *46*). In one such study, no difference in affinity for estradiol between the mouse wt receptor and the equivalent to Y537E was observed in receptor from transiently transfected COS cells (*28*). Another laboratory reported that the wt ER and the Y537S mutant from transiently transfected COS cells have a similar affinity for estradiol (*46*); this is similar to our observations using baculovirus-expressed receptor (Table 1). However, they observed a 3-fold slower dissociation rate for the Y537S mutant compared with the wt protein (*46*). Two factors are likely to account for the differences in results among laboratories. First, the stabilities of the receptor and its molecular form are sensitive to receptor concentration, salt concentration, temperature, and pH (*26*, *36*, *37*, *41*, *45*, *54*; Zhong and Skafar, unpublished observations). Our experiments were carried out in buffer containing 0.3 M NaCl, whereas others used a binding buffer containing low salt concentrations (*46*). Since biphasic dissociation kinetics or positive cooperative binding of the wt protein were not reported in the other studies, the receptors in those studies were most likely in the monomeric state (*46*). Also, the complement of coregulators and folding proteins is expected to differ between the COS cells and bacterial cells used for expression by others (*28*, *46*), and the *Sf9* cells used for expression in the present work. This could modify the conformation of the receptor and so contribute to the observed differences in the results.

Overall, the results of these and other studies show that Y537 plays a critical role in the stability of the receptor, its affinity for hormone, the kinetics of hormone binding, and the resulting transcription activation function of the receptor. These results are also consistent with the idea that the ligand follows different pathways for binding to and dissociating from the receptor. Additional studies on this interesting region of the protein are ongoing.

REFERENCES

1. Evans, R. M. (1988) *Science 240*, 889−895.
2. Parker, M. G. (1991) *Nuclear Hormone Receptors*, Academic Press, London.
3. Tsai, M. J., and O'Malley, B. W. (1994) *Annu. Rev. Biochem. 63*, 451−486.
4. Beato, M., Herrlich, P., and Schutz, G. (1995) *Cell 83*, 851−857.
5. Onate, S. A., Tsai, S. Y., Tsai, M. J., and O'Malley, B. W. (1995) *Science 270*, 1354−1357.
6. Voegel, J. J., Heine, M. J., Zechel, C., Chambon, P., and Gronemeyer, H. (1996) *EMBO J. 15*, 3667−3675.
7. Onate, S. A., Boonyaratanakornkit, B., Spencer, T. E., Tsai, S. Y., Tsai, M.-J., Edwards, D. P., and O'Malley, B. W. (1998) *J. Biol. Chem. 273*, 12101−12108.
8. Zeiner, M., and Gehring, U. (1995) *Proc. Natl. Acad. Sci. U.S.A. 92*, 11465−11469.
9. Suen, C. S., Berrodin, T. J., Mastroeni, R., Cheskis, B. J., Lyttle, C. R., and Frail, D. E. (1998) *J. Biol. Chem. 273*, 27645−27653.
10. Takeshita, A., Yen, P. M., Ikeda, M., Cardona, G. R., Liu, Y., Koibuchi, N., Norwitz, E. R., and Chin, W. W. (1998) *J. Biol. Chem. 273*, 21554−21562.
11. Xu, J., Qiu, Y., DeMayo, F. J., Tsai, S. Y., Tsai, M.-J., and O'Malley, B. W. (1998) *Science 279*, 1922−1925.
12. Norris, J. D., Fan, D., Stallcup, M. R., and McDonnell, D. P. (1998) *J. Biol. Chem. 273*, 6679−6688.
13. Katzenellenbogen, B. S., Fang, H., Ince, B. A., Pakdel, F., Reese, J. C., Wooge, C. H., and Wrenn, C. K. (1993) *Breast Cancer Res. Treat. 27*, 17−26.
14. Katzenellenbogen, J. A., O'Malley, B. W., and Katzenellenbogen, B. S. (1996) *Mol. Endocrinol. 10*, 119−131.
15. Smith, C. L., Nawaz, Z., and O'Malley, B. W. (1997) *Mol. Endocrinol. 11*, 657−666.
16. Tora, L., White, J., and Chambon, P. (1989) *Cell 59*, 941−951.
17. Webb, P., Nguyen, P., Valentine, C., Lopez, G. N., Kwok, G. R., McInerney, E., Katzenellenbogen, B. S., Enmark, E., Gustafsson, J. A., Nilsson, S., and Kushner, P. (1999) *Mol. Endocrinol. 13*, 1672−1685.
18. Bourguet, W., Ruff, P., Chambon, P., Gronemeyer, H., and Moras, D. (1995) *Nature 375*, 377−382.
19. Wagner, R. L., Apriletti, J. W., McGrath, M. E., West, B. L., Baxter, J. D., and Fletterick, R. J. (1995) *Nature 378*, 690−697.
20. Wurtz, J. M., Bourguet, W., Renaud, J. P., Vivat, V., Chambon, P., Moras, D., and Gronemeyer, H. (1996) *Nat. Struct. Biol. 3*, 87−94.
21. Brzozowski, A. M., Pike, A. C., Dauter, Z., Hubbard, R. E., Bonn, T., Engstrom, O., Ohman, L., Greene, G. L., Gustafsson, J. A., and Carlquist, M. (1997) *Nature 389*, 753−758.
22. Shiau, A. K., Barstad, D., Loria, P. M., Cheng, L., Kushner, P. J., Agard, D. A., and Greene, G. L. (1998) *Cell 95*, 927−937.
23. Tanenbaum, D. M., Wang, Y., Williams, S. P., and Sigler, P. B. (1998) *Proc. Natl. Acad. Sci. U.S.A. 95*, 5998−6003.
24. Williams, S. P., and Sigler, P. B. (1998) *Nature 393*, 392−396.
25. Skafar, D. F. (2000) *Cell Biochem. Biophys. 33*, 53−62.
26. Yudt, M. R., Vorojeikina, D. V., Zhong, L., Skafar, D. F., Sasson, S., Gasiewicz, T. A., and Notides, A. C. (1999) *Biochemistry 38*, 14146−14156.
27. Weis, K. E., Ekena, K., Thomas, J. A., Lazennec, G., and Katzenellebogen, B. S. (1996) *Mol. Endocrinol. 10*, 1388−1398.
28. White, R., Sjoberg, M., Kalkhoven, E., and Parker, M. G. (1997) *EMBO J. 16*, 1427−1435.
29. Zhang, Q. X., Borg, A., Wolf, D. M., Oesterreich, S., and Fuqua, S. A. (1997) *Cancer Res. 57*, 1244−1249.
30. Tremblay, G. B., Tremblay, A., Labrie, F., and Giguere, V. (1998) *Cancer Res. 58*, 877−881.
31. Tora, L., Mullick, A., Metzger, D., Ponglikitmongkol, M., Park, I., and Chambon, P. (1989) *EMBO J. 8*, 1981−1986.
32. Sasson, S., and Notides, A. C. (1983) *J. Biol. Chem. 258*, 8113−8117.
33. Scatchard, G. (1949) *Ann. N.Y. Acad. Sci. 51*, 660.
34. Henis, Y. L., and Levitzki, A. (1976) *Eur. J. Biochem. 71*, 529−552.
35. Hill, A. V. (1910) *J. Physiol. (London) 40*, iv−vii.
36. Weichman, B. M., and Notides, A. C. (1977) *J. Biol. Chem. 252*, 8856−8862.
37. Weichman, B. M., and Notides, A. C. (1979) *Biochemistry 18*, 220−225.
38. Obourn, J. D., Koszewski, N. J, and Notides, A. C. (1993) *Biochemistry 32*, 6229−6236.
39. Wyman, J., and Gill, S. J. (1990) *Binding and Linkage: Functional chemistry of biological macromolecules*, University Science Books, Mill Valley, CA.
40. Notides, A. C., Lerner, N., and Hamilton, D. E. (1981) *Proc. Natl. Acad. Sci. U.S.A. 78*, 4926−4930.

41. Notides, A. C., Sasson, S., and Callison, S. (1985) in *Molecular Mechanism of Steroid Hormone Action* (Moudgil, V. K., Ed.) pp 173−197, de Gruyter, New York.
42. Sauerwein, H., Pfaffl, M., Hagen-Mann, K., Malucelli, A., and Meyer, H. H. (1995) *Dtsch. Tierarztl. Wochenschr. 102*, 164−168.
43. Malayer, J. R. Submitted (JUL-1996) to the EMBL/GenBank/DDBJ databases.
44. Sack, J. S., Kish, K. F., Wang, C., Attar, R. M., Kiefer, S. E., An, Y., Wu, G. Y., Scheffler, J. E., Salvati, M. E., Krystek, S. R., Jr., Weinmann, R., and Einspahr, H. M. (2001) *Proc. Natl. Acad. Sci. U.S.A. 98*, 4904−4909.
45. Kosztin, D., Izrailev, S., and Schulten, K. (1999) *Biophys. J. 76*, 188−197.
46. Carlson, K. E., Choi, I., Gee, A., Katzenellenbogen, B. S., and Katzenellenbogen, J. A. (1997) *Biochemistry 36*, 14897−14905.
47. Gee, A. C., and Katzenellenbogen, J. A. (2001) *Mol. Endocrinol. 15*, 421−428.
48. Blondel, A., Renaud, J. P., Fischer, S., Moras, D., and Karplus, M. (1999) *J. Mol. Biol. 307*, 557−576.
49. Steinmetz, A. C., Renaud, J. P., and Moras, D. (2001) *Annu. Rev. Biophys. Biomol. Struct. 30*, 329−359.
50. Montano, M. M., Ekena, K., Krueger, K. D., Keller, A. L., and Katzenellenbogen, B. S. (1996) *Mol. Endocrinol. 10*, 230−242.
51. Arnold, S. F., Obourn, J. D., and Notides, A. C. (1995) *J. Steroid Biochem. Mol. Biol. 52*, 159−171.
52. Arnold, S. F., Vorojeikina, D. P., and Notides, A. C. (1995) *J. Biol. Chem. 270*, 30205−30212.
53. Arnold, S. F., and Notides, A. C. (1995) *Proc. Natl. Acad. Sci. U.S.A. 92*, 7475−7479.
54. Arnold, S. F., Melamed, M., Vorojeikina, D. P., Notides, A. C., and Sasson, S. (1997) *Mol. Endocrinol. 11*, 48−53.
55. Notides, A. C., and Nielsen, S. (1975) *J. Steroid Biochem. 6*, 483−486.

BI0121095